Journal of Physics Through Computation (2024)
Clausius Scientific Press, Canada

DOI: 10.23977/jptc.2024.060101
ISSN 2617-1163 Vol. 6 Num. 1

Role of pairing on transitional nuclei of the astrophysical interest

Sameena Murtaza[1,a,*]

[1]*Department of Physics, Lady Brabourne College, Park Circus, Kolkata, West Bengal, India*
[a]*sameenamurtaza55@gmail.com*
[*]*Corresponding author*

Keywords: Hartree-Fock-Bogoliubov, Skyrme Functional SLY6, Astrophysical r-process, Pairing Correlation, Deformation

Abstract: Hartreefock-Fock-Bogoliubov calculation have been done selfconsistently to study the shape transition and ground state properties namely binding energy, quadrupole deformation, hexadecapole deformation and charge radius of Platinum (Pt) isotopes from N=82 to N=126. We also study the effects of pairing force on the isotopes of transitional nucleus, Tungston. We use here Skyrme functional SLY6. We compare our results with experimental data wherever available and other studies in literature.

1. Introduction

Now a days, the structure of exotic nuclei and nuclei of astrophysical interest is a leading topic in nuclear structure studies. The number of exotic nuclei available away from the valley of stability are large in number and their structures are yet to be explored. Experimental data are not available for neutron dripline region due to limitations of experimental technique. Alternately, making reliable predictions for the ground state nuclear properties like binding energy, quadrupole deformation, hexadecapole deformation and charge radius of all nuclei in the periodic table is one of the interesting area of research in nuclear physics. Recent developments in experimental research like Radioactive Ion Beam (RIB) facilities have encouraged various theoretical physicist to explore the ground state (g.s) properties for nuclei of transition metals in the region far from the β stability line. Study of nuclear shapes of deformed nuclei is also a very interesting topic and a number of excellent review articles exist in this context [1], [2], [3]. The change of shape of nuclei from spherical to prolate, prolate to oblate then oblate to prolate and again spherical of nuclear structure with increase in neutron number have been investigated by different theoretical and experimental groups since many years [4], [5], [6]. In recent times some authors have studied the shape change of different nuclei [7], [4], [8]. Isotopic chains of Pt have been extensively studied, both experimentally and theoretically. For example, Mahapatro et. al. [9] have used the relativistic mean field formalism to study even-even dripline nuclei with Z = 70 to 80. Sarriguren et. al. [10] have studied shape transitions in neutron-rich Yb, Hf, W, Os and Pt isotopes within a Skyrme Hartree-Fock with BCS approach. Patra et. al. [11] have studied stable rare earth nuclei with A =160 to 230 in the relativistic mean field approach. Bassem et. al. [12] have also studied the shape evolution and the ground state properties of Pt isotopes with the help of covariant density functional theory. In spite of all these theoretical works, the role of

pairing has not been adequately investigated in neutron rich nuclei. Very often, pairing has been completely neglected in these calculations. However, as is well known, pairing significantly modifies ground state properties. In this work we will study effect of pairing strength on isotopic chain of Platinum then of Tungston.

Pt and W are important nuclei in r-process nucleosynthesis as the r-process abundance peak at A=195 corresponds to the N=126 closed neutron shell. In this work, we are interested to study shape transition and calculation of some ground-state properties like binding energy, quadrupole deformation, hexadecapole deformation and charge radii of even-even Pt and W isotopes having neutron number N=82 - 126 within the framework of Hartree-Fock-Bogoliubov (HFB) mean field theory with Skyrme functional SLY6. This paper is organized as follows: Hartree-Fock-Bogoliubov (HFB) mean field theory with Skyrme functional SLY6 and details of numerical calculations are given in section 2. Section 3 will cover our results. Finally, conclusion is given in section 4 followed by acknowledgement in section 5.

2. Theory and Calculation

2.1 HFB mean field theory

The standard Hartree-Fock theory is a reliable and successful theory in explaining the nuclear ground state properties of nuclei having closed shell near stability line, but it is not reliable for open shell nuclei far away from the stability where data are scarce. The standard Hartree Fock (HF) theory does not incorporate the pairing correlations. This non-inclusion of pairing correlations does not have large effect on closed shell nuclei as pairing vanishes in closed shell nuclei, but pairing effect is significant for nuclei which consist of open shells near the driplines. The pairing correlation generally incorporated with the help of the BCS approximation [13] for closed shell nuclei lying close to stability but BCS approximation becomes unreliable and collapses for ground state (g.s) properties as well as rotational states for nuclei lying close to the driplines. The Hartree-Fock Bogoliubov (HFB) includes pairing correlation self consistently. When there is no pairing effect, then HFB theory agrees with the result of the HF theory.

Following equation (1) and (2) are the HFB equations in terms of U and V transformation matrices where the quasiparticle energies e_n are the Lagrangian multipliers introduced to constrain the orthonormalization of the quasiparticle states. Here h is Gap Hamiltonians and Δ is pairing field. For more detail of HFB theory, see text.

$$\mathrm{H} \begin{pmatrix} U_n \\ V_n \end{pmatrix} = e_n \begin{pmatrix} U_n \\ V_n \end{pmatrix} \tag{1}$$

$$\mathrm{H} = \begin{pmatrix} h - \lambda & \Delta \\ -\Delta^* & -h^* + \lambda \end{pmatrix} \tag{2}$$

The calculation has been done using the publicly available code HFODD (ver 2.49T) by Schunck et. al. [14]. This code solves the HFB equations in a three dimensional deformed cartesian harmonic oscillator basis. Details of this code as well as the numerous equations that have been used in it, can be found in this reference as well as the references for earlier versions [15], [16], [17], [18], [19], [20]. The initial version of the code [19], [20] are important to understand the working of this code. There are various options for different energy functionals; we have chosen SLY6 [21]. In [21], a density dependent pairing was used and the same pairing strength was assumed for all the interactions from SLY4 to SLY7. The actual value of the strength depends upon the level density around the Fermi energy. In our calculation we have used a volume pairing term. Since pairing is expected to play an important role in our study, the pairing strength values for Pt isotopes have been chosen so as to reproduce the experimental value of binding energy and quadrupole deformation around the stable

isotopes. We use pairing strength for neutron and proton -249.8 MeV and -230.9 MeV respectively. We keep this strength constant throughout a large range of platinum isotopes but we have varied this pairing strength for Tungston isotopes. To observe the effect of pairing for Tungston isotopes, we have used the formula.

$$V_p = V_n = 124.66 + 3.88\ (N - 82) \quad (3)$$

In MeV, for the proton and neutron pairing strengths. We obtained this by comparing our results for the binding energy and deformation values with experimental measurements.

3. Results

In this section we present the results obtained in our work for Platinum and Tungston.

3.1 Binding Energy

Binding energy is a basic and important property in nuclear physics and is directly related to the stability of nucleus. We have calculated the binding energy of Platinum isotopes from $^{160-204}$Pt. Our results are satisfactory and in agreement with the results of Mahapatro et.al. [9]. Experimental values have been taken from the NNDC website [24]. We kept pairing strength constant for platinum isotopes. Pairing strength in our calculation for nuclei ^{160}Pt to ^{170}Pt do not reproduce the experimental values of binding energies but our results for these nuclei are very close to results of RMF[9]. Chosen pairing strength for these isotopes could be different. For the isotopes from ^{172}Pt to ^{178}Pt our results of binding energy are in fair agreement with experimental values as the chosen pairing strength fit for these isotopes and for rest of the isotopes from ^{180}Pt to ^{204}Pt our results of binding energy are in good agreement with experimental values as well as with FRDM[22]. Ground state binding energy of $^{160-204}$Pt isotopes is given in Table 1.

We have also calculated the binding energy for Tungston isotopes with different pairing strengths. Our results for binding energy are in good agreement with experimental results. From Table 4, it is seen that the binding energy values for Tungston isotopes differ from experimental measurements by less than 3 MeV. We have plotted the binding energy difference ΔE = B.E.(Exp.) - B.E.(Theo.)) for Tungston isotopes in Fig. 1. From the Figure 1 one sees that the binding energy values appear to be well described by our calculation.

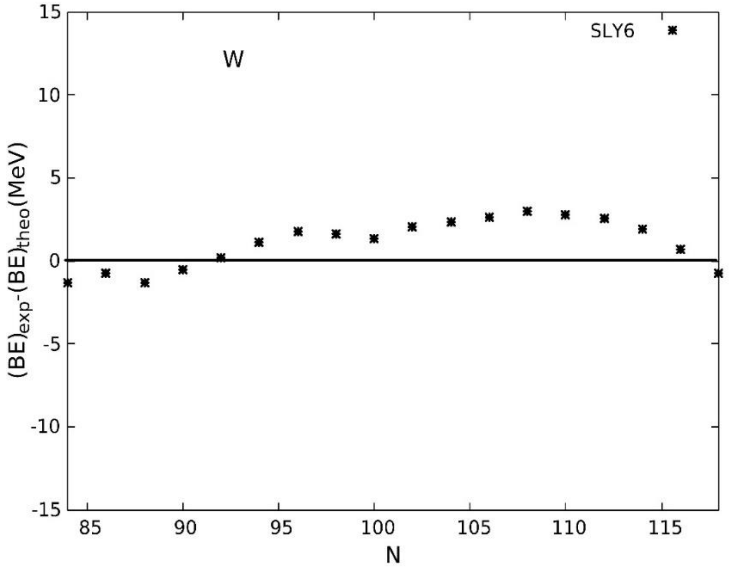

Figure 1: Difference between experimental and calculated binding energy values of W.

Table 1: Comparison of Binding Energy and charge radius of Pt isotopes with experimental data and other studies.

Isotope	BE(HFB)	BE(EXP)[24]	BE[9]	BE[22]	r_c(HFB)	r_c[33]	r_c[9]
^{160}Pt	-1222.348	-	-1222.1	-	5.20	-	5.24
^{162}Pt	-1246.888	-	-1246.0	-	5.21	-	5.25
^{164}Pt	-1269.992	-	-1268.2	-	5.23	-	5.27
^{166}Pt	-1292.163	-1283.678	-1290.3	-1283.8	5.24	-	528
^{168}Pt	-1313.619	-1306.015	-1310.0	-1305.6	5.26	-	5.30
^{170}Pt	-1334.475	-1327.405	-1332.0	-1327.2	5.28	-	5.31
^{172}Pt	-1354.737	-1348.340	-1351.3	-1348.2	5.30	-	5.36
^{174}Pt	-1374.348	-1368.704	-1372.2	-1368.7	5.31	-	5.39
^{176}Pt	-1393.326	-1388.462	-1392.3	-1388.5	5.33	-	5.41
^{178}Pt	-1411.715	-1407.668	-1411.7	-1407.9	5.35	5.37	5.43
^{180}Pt	-1429.506	-1426.249	-1430.6	-1426.4	5.38	5.39	5.45
^{182}Pt	-1446.686	-1444.124	-1448.8	-1444.4	5.38	5.40	5.46
^{184}Pt	-1463.232	-1461.438	-1465.7	-1461.9	5.39	5.40	5.47
^{186}Pt	-1479.147	-1478.106	-1481.6	-1478.5	5.40	5.40	5.48
^{188}Pt	-1494.675	-1494.212	-1496.2	-1493.5	5.41	5.41	5.48
^{190}Pt	-1509.710	-1509.852	-1510.0	-1509.1	5.42	5.41	5.48
^{192}Pt	-1524.258	-1524.962	-1524.3	-1524.2	5.43	5.42	5.46
^{194}Pt	-1538.146	-1539.575	-1538.9	-1539.0	5.43	5.42	5.45
^{196}Pt	-1551.425	-1553.602	-1552.8	-1553.2	5.44	5.43	5.46
^{198}Pt	-1564.394	-1567.003	-1566.3	-1566.8	5.45	5.44	5.46
^{200}Pt	-1577.206	-1579.842	-1579.6	-1580.0	5.45	-	5.47
^{202}Pt	-1589.458	-1592.075	-1592.5	-1592.5	5.46	-	5.47
^{204}Pt	-1600.745	-1603.440	-1605.3	-1604.1	5.47	-	5.48

3.2 Shape Transition and Quadrupole deformation

The quadrupole deformation is also an important property in nuclear physics which gives information about the shape of the nucleus. The quadrupole deformation parameter β_2 for the ground state for even-even isotopes of platinum $^{160-204}$Pt is obtained with nonrelativistic HFB theory with Skyrme functional SLY6. We plotted the potential energy surface (PES) of the platinum isotopes of $^{160-204}$Pt in Figure 2. The lightest isotopes, $^{160-162}$Pt shows spherical shape with deep minima. Next two isotopes $^{164-166}$Pt start to develop flat surface with small deformation 0.010 and 0.031 respectively. $^{168-184}$Pt isotopes show the pronounced prolate minima and an oblate local minima. Deformation values are given in Table 2. Isotope ^{186}Pt develops two degenerate minima oblate and prolate. Transition of shape occurs at ^{188}Pt with β_2, -0.127. From $^{190-198}$Pt isotopes show clear oblate shape. Prolate and oblate minima disappears for ^{200}Pt and shows flat surface. Isotope ^{202}Pt shows pronounced minima and ^{204}Pt a deep minima which confirms the spherical shape of the nucleus at magic number for neutron number N=126. Our results are in good agreement with FRDM [22] and [12], [25], [26], [27]. However calculation with different models shows different result which do not agree with our results, e.g Yao et.al. [28] where a beyond-mean-field approach with the Skyrme SLY6 predicts that the shape transition in Pt isotopes occurs at A = 186 to 188 instead of A = 188 as in our calculations. Constrained Hartree-Fock+ BCS calculations with the Skyrme forces Sk3, SGII and SLY4 by Boillos et.al. [29] suggest a prolate to oblate shape transition at A=182. Furthermore, ref [30] predicts a smooth shape transition at A = 184 to 186 by triaxial D1M-Gogny calculations. Mahapatro et. al.[9]

using RMF theory with pairing correlation from BCS approach (RMF-BCS) predicts the shape changes at ^{196}Pt. Different studies with different theoretical model and approaches show different results of shape transition.

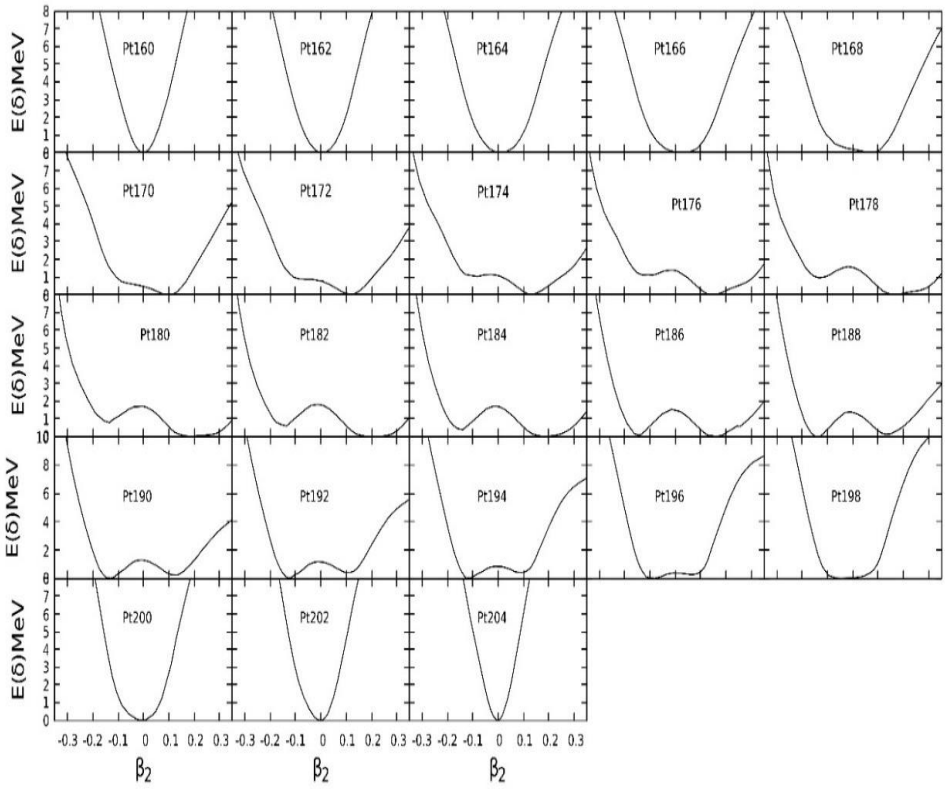

Figure 2: Potential energy surface (PES) of Pt Isotopes.

3.3 Charge Radius

Another important property of the ground state that has been measured is the charge radius. Charge radius could give the signals for the possibility of occurrence of new magic number or the disappearance of traditional magic number by taking into account the influence of shell effect on charge radius[31]. Nuclear charge radius is also useful for the study of neutron skin, neutron halo and isomer[31]. The charge radii (r_{ch}), in fm have been obtained from the root mean square point proton radius (r_p) using the formula

$$r_{ch} = \sqrt{r_P^2 + 0.64} \quad (4)$$

We have calculated the charge radii of $^{160-204}$Pt isotopes. We have compared our results of charge radii with experimental values [24] wherever available and also with RMF [9]. Our results for the nuclear charge radius are given in Table 1. Our results are in good agreement with experimental values and with RMF studies [9].

We have also calculated the nuclear charge radius for Tungston isotopes. In Table 4, we have shown our results for the charge radius of Tungston (W) isotopes and we have compared with experimental measurements and other study [9]. Experimental values of charge radii for Platinum and Tungston isotopes are from the compilation by Angeli and Marinova [31].

Table 2: Comparison of Quadrupole and Hexadecapole deformation of Pt isotopes with experimental data and other studies

Isotope	β_2(HFB)	β_2(EXP)[24]	β_2[9]	β_2[22]	β_4(HFB)	β_4[9]	β_4[22]
^{160}Pt	-0.000	-	-0.002	-	0.000	0.00	-
^{162}Pt	0.007	-	-0.00	-	0.000	0.00	-
^{164}Pt	0.010	-	-0.03	-	0.000	0.00	-
^{166}Pt	0.031	-	0.07	-0.07	0.000	0.00	-0.01
^{168}Pt	0.070	-	0.08	-0.10	0.002	-0.00	-0.01
^{170}Pt	0.089	-	0.09	0.11	0.001	-0.01	-0.00
^{172}Pt	0.119	-	0.25	0.13	0.002	0.09	-0.01
^{174}Pt	0.133	-	0.29	0.15	0.000	0.11	-0.01
^{176}Pt	0.145	0.189	0.31	0.17	-0.002	0.10	-0.01
^{178}Pt	0.176	-	0.32	0.25	0.003	0.08	0.01
^{180}Pt	0.192	0.252	0.32	0.27	0.003	0.05	-0.01
^{182}Pt	0.185	0.217	0.32	0.26	-0.007	0.03	-0.03
^{184}Pt	0.178	0.229	0.31	0.25	-0.015	0.01	-0.04
^{186}Pt	0.162	0.197	0.30	0.24	-0.023	-0.01	-0.06
^{188}Pt	-0.127	0.191	0.28	-0.16	-0.001	-0.03	-0.01
^{190}Pt	-0.129	0.152	0.25	-0.16	-0.003	-0.05	-0.02
^{192}Pt	-0.122	0.153	0.18	-0.16	-0.006	-0.06	-0.03
^{194}Pt	-0.109	0.142	0.14	-0.15	-0.008	-0.06	-0.03
^{196}Pt	-0.080	0.129	-0.13	-0.14	-0.007	-0.03	-0.03
^{198}Pt	-0.043	0.114	-0.11	-0.14	-0.003	-0.02	-0.03
^{200}Pt	-0.002	-	-0.08	-0.09	-0.001	-0.03	-0.03
^{202}Pt	0.000	-	-0.00	-0.06	-0.000	0.00	-0.04
^{204}Pt	-0.000	-	0.00	0.01	-0.000	0.00	0.00

3.4 Hexadecapole deformation

We have also calculated the hexadecapole deformation for the $^{160-204}$Pt isotopes and our results are shown in Table 2. We compared our results with RMF [9] and FRDM [22]. Hexadecapole deformation is zero for isotopes N=82, 84, 86 and 88. It changes sign at N=98 then becomes positive and again negative and become zero for the isotopes N=124 and 126. We are getting smaller hexadecapole deformation as compared to RMF and FRDM. Hexadecapole deformation of Tungston isotopes are given in Table 3. Hexadecapole deformation first decreases from N=84 then increases from N=94. It again decreases from N=102 and become negative at N=106. For Tungston isotopes we obtained small values.

Table 3: Hexadecapole deformation of few representative of Tungston isotopes.

Isotope	β_4	Isotope	β_4	Isotope	β_4
^{158}W	0.0498	^{168}W	0.0326	^{178}W	0.0206
^{160}W	0.0491	^{170}W	0.0753	^{180}W	-0.0040
^{162}W	0.0498	^{172}W	0.0952	^{182}W	-0.0242
^{164}W	0.0299	^{174}W	0.0859	^{184}W	-0.0381
^{166}W	0.0132	^{176}W	0.0547	^{186}W	-0.0415

Table 4: Comparison of Binding Energy, Quadrupole deformation and charge radius of W isotopes with experimental data.

Isotope	BE(HFB)	BE(EXP) [24]	β_2(HFB)	β_2(EX) [24]	r_c(HFB)	r_c[33]
^{158}W	-1242.430	-1241.1	0.122	-	5.178	-
^{160}W	-1263.658	-1262.9	0.158	-	5.202	-
^{162}W	-1284.990	-1283.7	0.186	-	5.225	-
^{164}W	-1304.528	-1304.0	0.193	-	5.241	-
^{166}W	-1323.635	-1323.8	0.200	-	5.259	-
^{168}W	-1341.884	-1343.0	0.222	0.23	5.279	-
^{170}W	-1359.751	-1361.5	0.268	0.24	5.314	-
^{172}W	-1377.894	-1379.5	0.313	0.28	5.356	-
^{174}W	-1395.341	-1396.7	0.326	0.25	5.378	-
^{176}W	-1411.274	-1413.3	0.305	-	5.377	-
^{178}W	-1426.862	-1429.2	0.280	-	5.377	-
^{180}W	-1441.943	-1444.6	0.265	0.25	5.384	5.3491
^{182}W	-1456.331	-1459.3	0.251	0.25	5.392	5.3559
^{184}W	-1470.134	-1472.9	0.237	0.24	5.399	5.3658
^{186}W	-1483.357	-1485.9	0.216	0.23	5.402	5.3743
^{188}W	-1496.279	-1498.2	0.186	-	5.401	-
^{190}W	-1509.202	-1509.9	0.156	-	5.401	-
^{192}W	-1522.145	-1521.4	0.129	-	5.404	-
^{194}W	-1535.120	-	0.104	-	5.409	-
^{196}W	-1547.792	-	0.091	-	5.419	-
^{198}W	-1560.211	-	0.081	-	5.429	-
^{200}W	-1571.583	-	0.01	-	5.448	-

4. Conclusion

Ground state properties of Platinum and Tungston isotopes have been studied in the HFB mean field approach using the energy functional SLY6 in the present work. Pairing strength has been obtained by fitting the binding energy and quadrupole deformation with experimental values. Pairing strength has been kept constant for Platinum isotopes. The results obtained are in fair agreement with experimental values and other studies for ground state properties such as binding energy, quadrupole deformation, hexadecapole deformation and charge radius. Potential energy surface is also studied for the shape transition which is also in good agreement with results obtained in other studies. Lighter isotopes are prolate in shape while shape transition occurs at N=110. Spherical shape have been confirmed for N=82 and N=126. Our results are in good agreement with other studies and experimental values wherever available. We have also performed the unrestrained calculation for the g.s properties of Tungston isotopes. Pairing strength has been varied for Tungston isotopes as a simple function of neutron numbers to reproduce the binding energy and deformation values. Good agreement has been obtained for binding energy, charge radii, quadrupole deformation and hexadecapole deformation in the ground state for Tungston isotopes as well as Platinum isotopes except for few Platinum isotopes. Role of pairing is important in order to produce ground state properties of deformed nuclei therefore a more systematic study is required to understand the g.s properties of exotic nuclei which are vital in r- process. We intend to carry out rotational solution for exotic nuclei with more realistic nuclear astrophysical model with different Skyrme functional. High

spin state calculation of transitional nuclei is also required to understand more precisely astrophysical r- process of nucleosynthesis. Systematic calculation of r- process nuclei with N=50, 82 and N=126 closed shell has to be performed for better understanding of required condition for nucleosynthesis of r process nuclei in Solar pattern.

Acknowledgements

Author expresses sincere gratitude to her supervisors Prof. G. Gangopadhayay and Prof. Abhijit Bhattacharyya, Department of Physics, University of Calcutta, West Bengal. Prof. G. Gangopadhayay has helped and advised during this research work. Author also gratefully acknowledges the opportunities provided by Lady Brabourne College authorities to carry out this work.

References

[1] P. J. Nolan and P. J. Twin (1988), Superdeformed Shapes at high Angular Momentum, Annu. Rev. Nucl. Part. Sci. 38, 533. https://doi.org/10.1146/annurev.ns.38.120188

[2] S. Aberg et al. (1990), Nuclear Shapes in mean field theory, Annu. Rev. Nucl. Part. Sci. 40, 439. https://doi.org/10.1146/annurev.ns.40.120190.

[3] C. Baktash et al. (1995), Identical Bands in deformed and Superdeformed Nuclei, Annu. Rev. Nucl. Part. Sci. 45, 485.doi 10.1146/annurev.ns.45.120195.002413

[4] P. Quentin and H. Flocard, (1978), Self-Consistent Calculations of Nuclear Properties with Phenomenological Effective Forces, Annu. Rev. Nucl. Part. Sci. 28, 523. https://doi.org/10.1146/annurev.ns.28.120178.002515.

[5] M. Baranger and K. Kumar (1968), Nuclear deformations in the Pairing-plus quadrupole Model: (II). Discussion of validity of the model, Nucl. Phys. A 110, 490. https://doi.org/10.1016/0375-9474 (68)90370-9

[6] G. D. Alkhazov et al. (1989), Nuclear deformation of Holmium Isotopes, Nucl. Phys. A 504, 549. https://doi.org/10.1016/0375-9474(89)90557-5.

[7] S. K. Patra and P. K. Panda (1993), Systematic study of neutron deficient Ho isotopes in a relativistic mean field theory, Phys. Rev. C 47, 1514. https://doi.org/10.1103/PhysRevC.47.1514

[8] M. M. Sharma and P. Ring (1992), Relativistic mean field description of neutron deficient platinum isotopes, Phys. Rev. C 46, 1715. https://doi.org/10.1103/PhysRevC.46.1715.

[9] S. Mahapatro et al. (2016), Nuclear structure and decay properties of even-even nuclei in Z = 70 - 80 drip line region, Int. Jour. Mod. Phys. E 25, 1650062. https://doi.org/10.1142/S0218301316500622.

[10] P. Sarriguren et al. (2008), Shape transitions in neutron-rich Yb, Hf, W, Os and Pt isotopes within a Skyrme-Hartree-Fock + BCS approach, Phy. Rev. C 77, 064322. https://doi.org/10.1103/PhysRevC.77.064322.

[11] S. Patra et al. (1999), Oscillation in deformation properties of heavy rare earth nuclei, J. Phys. G. 25, 501. https://doi.org/10.1088/0954-3899/25/3/003.

[12] Y. E. Bassem and M. Oulne (2019), Ground state properties and shape evolution in Pt isotopes within the covariant density functional theory, Int. Jour. Mod. Phys. E 28, 1950078. https://doi.org/10.1142/S0218301319500782

[13] J.Bardeen et al. (1957), Theory of Superconductivity, Phys. Rev. 108, 1175. doi:https://doi.org/ 10.1103/PhysRev.108.1175.

[14] J. Dobaczewski et al. (2009), Solution of the Skyrme-Hartree-Fock-Bogolyubov equations in the Cartesian deformed harmonic-oscillator basis: (VI) HFODD (v2.40h), Comp. Phys. Comm. 180, 2361. doi:10.1016/j.cpc.2009.08.009.

[15] N. Schunck et al. (2012), Solution of the Skyrme-Hartree Fock-Bogolyubov equations in the Cartesian deformed harmonic-oscillator basis:(VII) HFODD (v2.49t) Comp. Phys. Comm. 183, 166.

[16] J. Dobaczewski and P. Olbratowski (2005), Solution of the Skyrme-Hartree-Fock Bogolyubov equations in the Cartesian deformed harmonic-oscillator basis. (V) HFODD(v2.08k), Comp. Phys. Comm. 167, 214. https://doi.org/10.1016/j.cpc.2005.01.014.

[17] J. Dobaczewski and P. Olbratowski (2004), Solution of the Skyrme-Hartree-Fock Bogolyubov equations in the Cartesian deformed harmonic-oscillator basis. (IV) HFODD (v2.08i), Comp. Phys. Comm. 158, 158. https://doi.org/10.1016/j.cpc.2004.02.003.

[18] J. Dobaczewski and J. Dudek (2000), Solution of the Skyrme-Hartree-Fock equations in the Cartesian deformed harmonic-oscillator basis. (III) HFODD (v1.75r), Comp. Phys. Comm. 131, 164. https://doi.org/10.1016/S0010-4655 (00)00121-1.

[19] J. Dobaczewski and J. Dudek (1997), Solution of the Skyrme-Hartree-Fock equations in the Cartesian deformed harmonic oscillator basis I. The method, Comp. Phys. Comm. 102, 166. https://doi.org/10.1016/S0010-4655

[20] J. Dobaczewski and J. Dudek (1997), Solution of the Skyrme-Hartree-Fock equations in the Cartesian deformed harmonic oscillator basis II. The program HFODD, Comp. Phys. Comm. 102, 183. https://doi.org/10.1016/S0010-4655 (97)00005-2.
[21] E. Chabanat et al. (1998), A Skyrme parametrization from subnuclear to neutron star densities Part II. Nuclei far from stabilities, Nucl. Phys. A 635, 231. doi: 10.1016/S0375-9474(98)00180-8.
[22] P. Moeller et al. (1997), Nuclear Properties for Astrophysical and Radioactive ion beam Application, Atom. Nucl. Data Table 66, 131. doi:10.1006/adnd.1997.0746.
[23] P. Moeller et al. (1995), Nuclear Ground State Masses and Deformations, Atom. Nucl. Data Table 59, 185. https://doi.org/10.1006/adnd.1995.1002.
[24] https://www.nndc.bnl.gov, NuDat3.0 (2023).
[25] R. Rodriguez-Guzman et al. (2010), Mean field study of structural changes in Pt isotopes with the Gogny interaction, Phys. Rev. C 81, 024310. https://doi.org/10.1103/PhysRevC.81.024310.
[26] J.-E. Garcia-Ramos et al. (2014), Shape evolution and shape coexistence in Pt isotopes: Comparing interacting boson model configuration mixing and Gogny mean field energy surfaces, Phys. Rev. C 89, 034313. https://doi.org/10.1103/PhysRevC.89.034313.
[27] K. Nomura et al. (2011), Structural evolution in Pt isotopes with the interacting boson model Hamiltonian derived from the Gogny energy density functional, Phys. Rev. C 83, 014309. https://doi.org/10.1103/PhysRevC.83.014309.
[28] J. Yao et al. (2013), Systematics of low-lying states of even-even nuclei in the neutron deficient lead region from a beyond-mean field calculation, Phys. Rev. C 87, 034322. 10.1103/Physrevc.87.034322.
[29] J. M. Boillos and P. Sarriguren (2015), Effects of deformation on the decay patterns of light even-even and odd-mass Hg and Pt isotopes, Phys. Rev. C 91, 034311. https://doi.org/10.1103/PhysRevC.91.034311.
[30] K. Nomura et al. (2013), Shape evolution and the role of intruder configurations in Hg isotopes within the interacting boson model based on a Gogny energy density functional, Phys. Rev. C 87, 064313. https://doi.org/10. 1103/PhysRevC.87.064313.
[31] I. Angeli and K. Marinova (2013), Table of experimental nuclear ground state charge radii: An Update, Atom. Data Nucl. Data Tables 99, 69. doi.10.1016/j.adt.2011.12.006.